Early-establishment population dynamics of an aquatic invader (*Procambarus clarkii*) in replicated pond ecosystems

Emma Sofia Embla Hellem

Master of Science in Marine Biology and Limnology

Department of Bioscience, Center of Ecological and Evolutionary Synthesis

University of Oslo, Norway

August 2023

Abstract

While invasive species obtain widespread attention for their ecological implications, the earlier stages of their invasion usually remain as uncharted territory. *Procambarus clarkii* is well known for being one of the most successful invaders worldwide, and yet little is known of how the population and its individuals are affected by the environment during the initial establishment. Therefore, this project has focused on investigating the role of density- and temperature- dependent factors influencing the population growth rate and somatic growth rate of *P. clarkii* in replicated self-sustained mesocosms.

A state-space model revealed that temperature and density play a significant role in in population dynamics of the crayfish, where high temperatures and high density resulted in a large population increase during spring. Meanwhile, high competition and low resource availability in the following summer led to a population crash. Key findings from a linear mixed-effects model revealed that the significant influence of density and temperature on somatic growth rate suggested a possible ripple effect on the dynamics of population growth rate. Additionally, it was suggested that crayfish somatic growth was rescued as the crayfish grew larger, and that ecology may have a stronger effect on somatic growth than physiology. Lastly, both sex and crayfish size seamed to play a role in energy allocation, due to the hierarchical nature of *P. clarkii.*

Acknowledgements

The last two years have been an amazing new chapter in my life and being a master student have tough me so much about the vast field of biology. Writing this master have been an exciting challenge and I am proud of my accomplishments. I am happy to have had this opportunity and to share my experiences alongside my supervisors, friends, and family.

Thank you to AQUACOSM-plus for their generous financing support, which made this project possible. Their funding extended beyond the project itself, by facilitate the traveling and housing for both me and my colleagues, making fieldwork in Rennes possible.

Thank you to my internal supervisor, Leif Asbjørn Vøllestad, for always offering a helping hand no matter the magnitude of my never-ending questions. I am really grateful for all your guidance and hours spent in your office discussing crayfish, and for always pushing me to keep going. Thank you to my external supervisor, Eric Edeline. You have taught me so much and really sparked my passion for crayfish! Your waste knowledge of statistics goes above and beyond, and I thank you for sharing it with me. I have really learned a lot! Your work on making the CMR data into estimated population numbers created a solid foundation of date which were then available for me to use. It is thanks to you that I was able to crate my own models and peruse the statistical aspects of this project to its extent.

To my classmates, Emma, Jacquelynn, and Mari, thank you for helping me with field work in Rennes. Your contribution to the project, as well as your warm kindness and excitement gave me encouragement and happiness, and I had a blast experiencing this together. And thank you to my marine classmates. We have helped each other throughout good and bad, and I am forever thankful for all the times we have spent together.

A heartfelt thank you to my family for their endless support and encouragement. Thank you for always being my unwavering sidekicks cheering for me while I explore uncharted territories of life (and crayfish).

Table of Contents

INTRODUCTION

Invasive species, a well-known environmental challenge, have for the last two decades gained considerable attention due to the large negative impact they cause worldwide. An invasive species is a non-native species that causes environmental harm or harm to humans when introduced to a new area (Rutledge et al., 2022). It easily adapts to the new environment and quickly reproduces. When an invasive species establishes itself, it often displaces native species, changes the biodiversity, permanently alters the habitat, and may even dominate it. Invasive species typically cause three types of damage: economical (economic loss, management and control cost), damage to the ecosystem, and damage to human health (*NISIC*, 2023). Invaders are one of the biggest threats to biodiversity (Doherty et al., 2016; Molnar et al., 2008) and specially represent a big threat to freshwater environments (Havel et al., 2015; Keller et al., 2011).

Figure 1: Adult *Procambarus clarkii.* Photo: Eric Edeline.

Among these invaders, freshwater crayfish are known for being some of the most invasive freshwater organisms on a global scale, and have been showed to alter multiple environmental components in their habitat even at low density levels (Galib et al., 2022). The red swamp crayfish (*Procambarus clarkii*, Girard 1852) is considered as one of the most invasive species worldwide (Fig. 1). Native to Louisiana (USA), it has rapidly spread too all continents (except Antarctica) (Oficialdegui et al., 2019), due to economical values in the food industry and its elevated adaptive capabilities (Loureiro et al., 2015). There is a great concern regarding the intensive introduction of *P. clarkii* as it has specific features that favors its colonization success across different climatic and geographic areas. Some of these features are its ecological plasticity, resistant gene pool to population changes, adaptation of its biology and life cycle to changing environmental conditions, high tolerance to salinity, oxygen and temperature variations, high somatic growth and reproductive output, short development time and flexible feeding strategy (Alcorlo et al., 2004; Gherardi, 2006; Jones et al., 2009). Additional, *P. clarkii* has a wide adaptability to a variety of freshwater habitats, including rivers, swamps and marshes, ponds, lakes, and rivers. It is a successful colonizer that quickly establishes itself in new habitats and takes over the role as a key stone species, the primary contributor to its inhabited food-web (*Global Invasive Species Database*, 2023). Once introduced to a favorable habitat, it becomes quite difficult to eliminate (Holdich, 1988). Additionally, the crayfish has been shown to make extensive changes to plant and animal communities and outcompete native crayfish species through direct competition and spread of diseases and parasites (Gherardi, 2007; Loureiro et al., 2015).

Despite its invasion capability (and popularity in aquaculture), only a few studies have been done to investigate their establishment, especially in the earlier phases. Establishment of an invasive species

happens between the initial introduction and the integration of the invader into the receiving ecosystem (Crooks & Rilov, 2009). Most available information concerns already successful invaders. This makes it hard to distinguish between factors that operate in the introduction and establishment phase. Therefore, the question of when and how an invader fails poorly studied. Generally, less is known about unintentionally introduced species because they are not recorded until they already have become established (Keller et al., 2011). Additionally, early stages of invasion are often difficult or impossible to detect, partly due to limitations in methods of investigation. Also, slow spread is usually not detectable with regular surveys, and it is hard to capture crayfish in their natural habitat and due to their cryptic nature. Similarly, they are hard to detect at low densities (Holdich & Sibley, 2003).

Furthermore, little is known about how the invader and the receiving environment affect each other in the early phases of invasion. Both ecological and physiological factors play a role in how the crayfish relate to their environment and will ultimately affect the population growth rate as well as the individual (somatic) growth rate. It is well documented that factors like temperature and density have a significant impact on these growth rates in aquatic organisms by influencing metabolic rates, competition, and resource availability. These elements are vital for an organism's growth and overall success in an ecosystem.

Therefore, this project focused on investigating the contribution of density- and temperature-dependent processes to crayfish population dynamics of *P. clarkii* during the early phases of invasion. Capture Mark Recapture (CMR) methods were used to follow individual growth trajectories and to estimate the population size of crayfish populations over time in replicated self-sustained mesocosms. Modeling of population dynamics was conducted using a state-space model for stochastic population growth, meanwhile individual somatic growth was modeled using a linear mixed effects model. This study will thus contribute to increasing our understanding of ecological processes influencing the crayfish populations under the first stage of invasion, namely establishment.

MATERIAL AND METHODS

This project was part of a long-term mesocosm experiment taking place at the U3E experimental unit in Rennes, France (https://eng-u3e.rennes.hub.inrae.fr/). This experiment includes monitoring of crayfish, but also of macrophytes, macroinvertebrates and plankton. It is being run by the DECOD laboratory (https://www.umr-decod.fr/en), located in Rennes, France. The program focuses on observing and understanding how invasive species of crayfish impact freshwater ecosystems. Central themes in this project are changes in food-web structure, eco-evo feedbacks and consequences to

ecosystem function and stability. The project started in 2020, with installation of 12 mesocosms (see below). Since 2020, a routine monitoring of macrophyton, periphyton, phyto- and zooplankton and macroinvertebrates have been performed (monthly since January 2021). In June 2021, the experiment really started with the introduction of red crayfish. 40 crayfish were mixed in equal proportions from two different populations and locations: Brière Marsh (near St Nazaire, NO France) and from Lamartine Lake near Toulouse, SO France (10 males + 10 females from each location in each mesocosm). The experiment is thought to run until the end of 2027.

Study species

Crayfish belong to the phylum Arthropoda and under the order Decapoda (Longshaw & Stebbing, 2016). The study species *P. clarkii* was first described by Girard, C.F. (1852) previously known by its synonymized name *Cambarus clarkii.* The body morphology is of a typical decapod crustacean being divided into a cephalothorax and abdomen where both have appendages that follow the decapod pattern (Hobbs & Horton, 1974). Both males and females have pleopods (abdominal appendages) which are not usually present in decapod males. Sex differentiation can be done by looking at external organs. Males' first abdominal appendages are transformed into copulatory organs, the gonopodiums (Fig. 2b,c). Females' first abdominal appendages are vestigial. Females also have more developed posterior abdominal appendages, and have a copulatory receptacle as well as *annulus ventralis* (Fig. 2a) (J. Huner, 2018). Total body length can be up to 15 cm in length (Loureiro et al., 2015), however, this tend to variate among individuals and population.

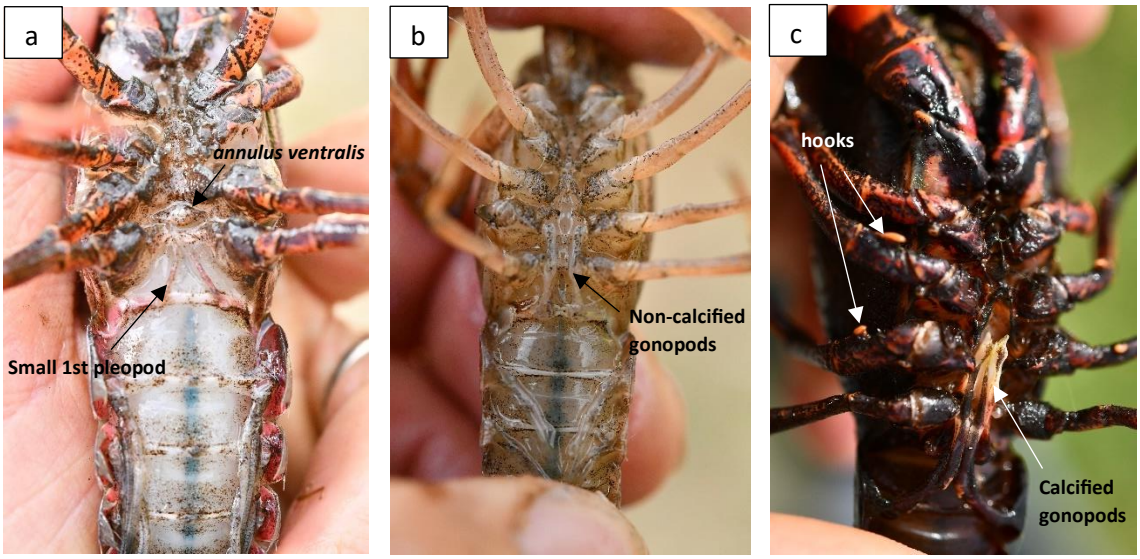

Figure 2: Ventral view of *Procambarus clarkii* individuals. a: Female showing the first pair of abdominal appendages (pleopods) that are vestigial and the *annulus ventralis* (copulatory hole). b: Morphotype I male (non-reproductive form) showing the softened copulatory organs (gonopods) and the pereiopods with no hooks. c: Morphotype II male (reproductive form) showing calcified copulatory organ and pereiopods with hooks on the 3rd and 4th pair of walking legs. Photos: Eric Edeline (A, C) and Emma Hellem (B).

P. clarkii has sexual reproduction and can produce 2-3 generations per year (depending on climate). Males alternate between 2 morphotypes, with and without copulating hooks. Females have fixed morphotype, but they have a reproductive state where they bear eggs with holding pods underneath their tails (Loureiro et al., 2015).

Crayfish inhabit shallow waters and marshes ranging anywhere between freshwater to brackish water. Younger individuals are usually found in deeper waters (down to approx. 1 m) and will with maturity start to venture out to more open waters (less than approx. 15 cm) (Penn, 1943). The presence of crayfish can typically be recognized through shallow muddy water and uprooted aquatic plants. *P. clarkii* are most active at night and during sunny days they hide under surface-floating vegetation and in burrows (Penn, 1943). From these points they move to open waters to find food or mates. On cloudy and rainy days, they are more active, and only disabled or newly molted individuals stay hidden (Penn, 1943).

Study area

Crayfish were present in 8 mesocosms and absent from 4 mesocosms used as controls for ecosystem-related aspects of the experiment. Mesocosms were localized in an open outside field on the premises of the research facility (figure 3). Each mesocosm was 3.7 x 1.5 m in size and were placed approximately 2-3 m apart. Each mesocosm was filled with approximately 0.55 m^3 of pond sediments forming a 5 cm bottom layer (on all surface). The pond sediments were collected from local ponds which contained propagules from plants and animals. From these propagules, the vegetation established fast (Fig. 4a) but was quickly eaten by the crayfish (Fig. 4b). In the following spring, 45 snails (*Lymnaea stagnalis*) from a mixture of strains maintained in the U3E lab were added in all mesocosms.

The mesocosms were initially filled with city tap water from the research station. A constant water level was maintained by letting excess water run through an overflow, and tap water was added when needed to maintain water level in between.

Temperature loggers were placed in mesocosm 1, 6, 10 and 12, recording the temperature hourly since December 2020 and continuing until the end of the project (Fig. 5). For the analysis, mean hourly surface temperature was computed during the transition interval between two capture occasions.

During the project, the condition of the mesocosm seamed to decrease. Plants were mostly gone by May 2022, and by the same time, the water of some of the mesocosm had started to become murky. Throughout the summer, this water condition was observed in all the mesocosm, and by August, the

water had become ill-smelling (Fig. 4B). Insects and snails were harder to monitor but seemed to decline with the plants and water quality simultaneously.

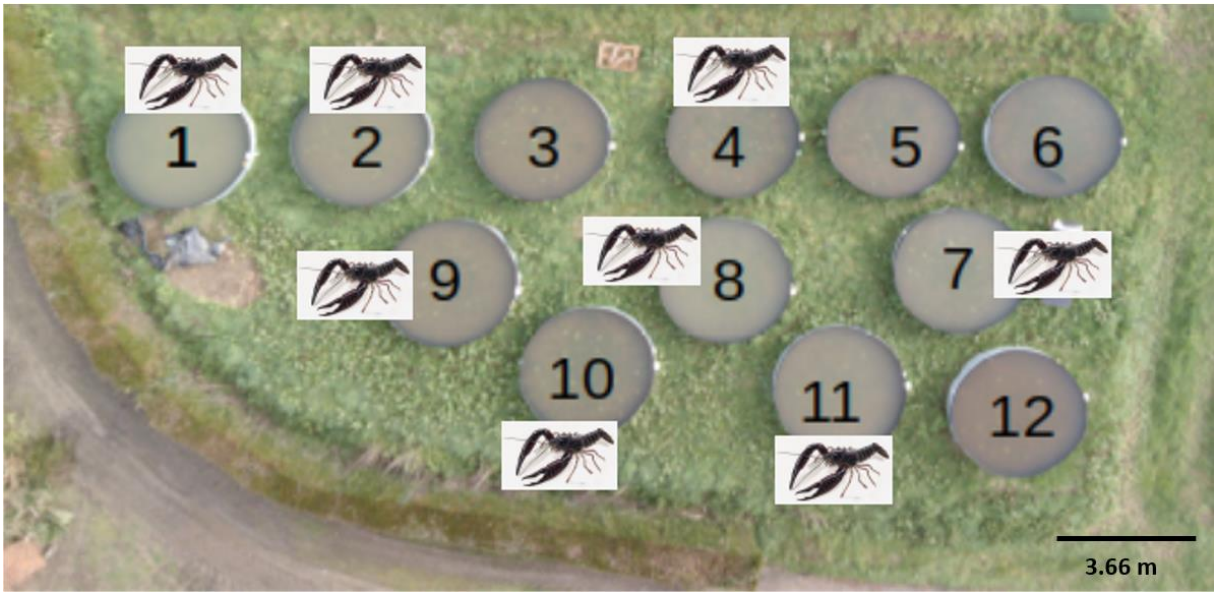

Figure 3: The project took place on an open grass field in the research facility of INRAE Brittany-Normandy center located in Rennes, France with 8 mesocosms with crayfish (1, 2, 4, 7, 8, 9, 10, 11) and 4 control tanks without crayfish (3, 5, 6, 12).

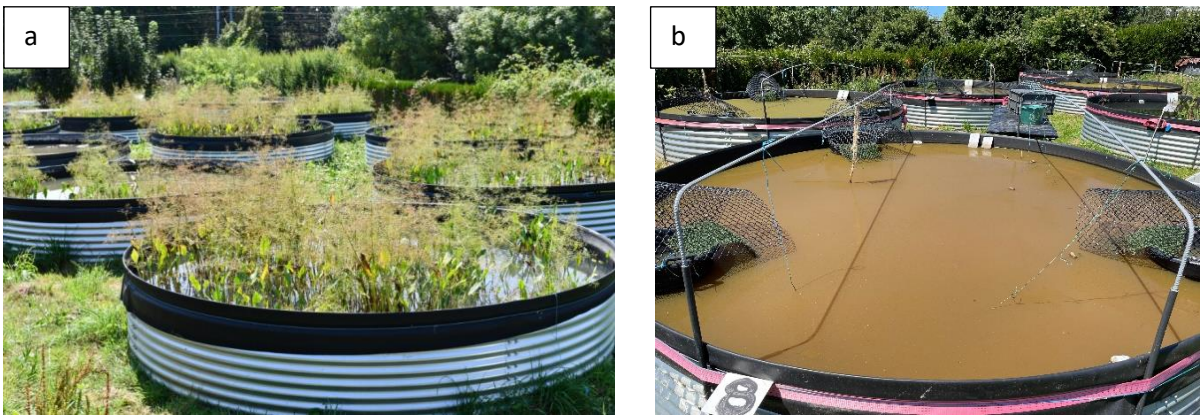

Figure 4: Mesocosms (a) before introduction in August 2020 of crayfish with clear water and full of vegetation, and (b) after introduction in June 2022 where the water has become murky and brown with no vegetation. Photos: Eric Edeline (a) and Emma Hellem (b).

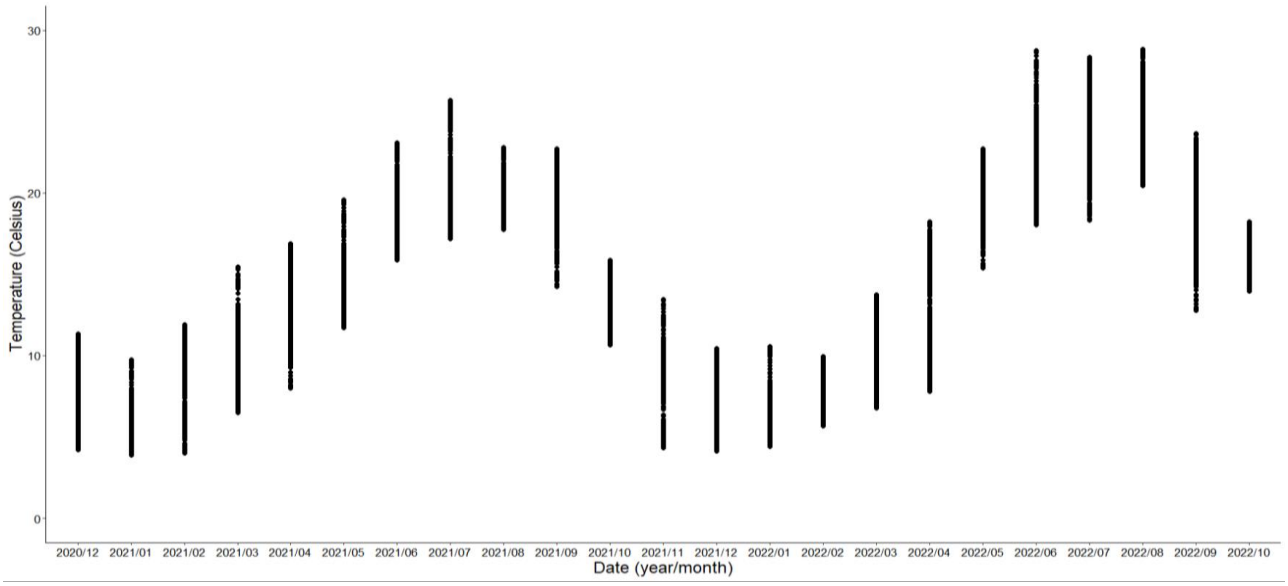

Figure 5: Monthly range of surface water temperatures throughout the project, measured in mesocosm 1 and obtained from logger measurements.

Experimental design

Introductions of the crayfish took place in June 2021 where each of the 8 mesocosms received exactly 40 crayfish (20 large adult males and 20 large adult females in each), so the 8 mesocosms can be considered as 8 replicates of the same treatment (Fig. 3).

At introduction, all crayfish were phenotyped (see "Biometric method" below) and tagged ventrally with Passive Integrated Transponder (PIT) tags (8 mm x 1.4 mm PIT-tags) into the tail musculature (left part of the 3rd abdominal segment). The 8 crayfish populations were subsequently monitored using individual capture-mark-recapture (CMR) during 5 primary CMR occasions in total: October 2021, May 2022, June 2022, August 2022, and October 2022. A "robust design" was applied, involving 5 secondary occasions (Monday to Friday) during each primary occasion. Assuming no birth or death during these 5 consecutive days, the robust design allows estimation of separate capture probability and population numbers at each primary occasion and mesocosm (Williams et al., 2002). The CMR data was used by one of the supervisors of this project, to estimate population numbers for each occasion (see "Population analysis" below) using a hierarichial spatial CMR model of the type sescribed by Role & Converse (2014). These population number estimates were then used as "data" for further analysis in this project.

Captured non-tagged crayfish with a total body length ≥ 55 mm were tagged with the PIT-tags. Individuals that were accidentally tagged twice were removed from the project as the tag could no longer be read.

Crayfish of 20 mm ≤ total length ≤ 54 mm were too small for PIT-tags and therefore marked with nail polish instead. The cephalothorax was dried with paper and two dots of nail polish (for reassurance in case one fell off) were placed on either side of the cephalothorax (see Appendix A). A new color was used every day to distinguish which dates the individual had been caught/not caught. Each new color was placed posterior to the prior color. Crayfish with a total length < 20 mm were not phenotyped or tagged at all.

Five different trap types were used to capture individuals. The different traps were chosen to capture crayfish with different sizes and behaviors. Artificial Refuge Traps (ART, 5 entrances with a 26.5 or 32.5 mm inner-tube diameter, Fig. 6a) were meant to catch individuals displaying hiding- and burrowing behaviors. Smaller versions of the ART and small plastic tubes were added into the other trap types to provide shelter for the smaller individuals and prevent antagonistic behavior and cannibalism. Exit traps (ET, with protective (plastic) mesh covering the trap, Fig. 6b) would capture crayfish that displayed the behavior of exiting the water. Fine Mesh Traps (FMT, 2 mm (nylon) mesh and 2 entrances with a 4 cm opening, Fig. 6c), with the capacity of capturing all sizes, were primarily aimed at juveniles. Coarse mesh traps (CMT, 2 cm (metal) mesh and 2 entrances with a 4 cm opening, Fig. 6d) were targeting the largest crayfish, and finally medium mesh traps (MMT, 5 mm (metal) mesh and 2 entrances with a 4 cm opening, Fig. 6d) were meant to replace 8 missing CMTs.

In total, 21 traps were placed in each of the 8 mesocosm which contained crayfish: 3 FMT, 12 ART, 3 CMT (2 from June 2022), and 3 Exit traps. One MMT was added in each mesocosm in June 2022. To ensure thorough sampling of each crayfish size and behavior type, a uniform distribution of each trap type was implemented throughout each mesocosm. All traps were set on Friday afternoon and sampled every day in the following week (Monday – Friday).

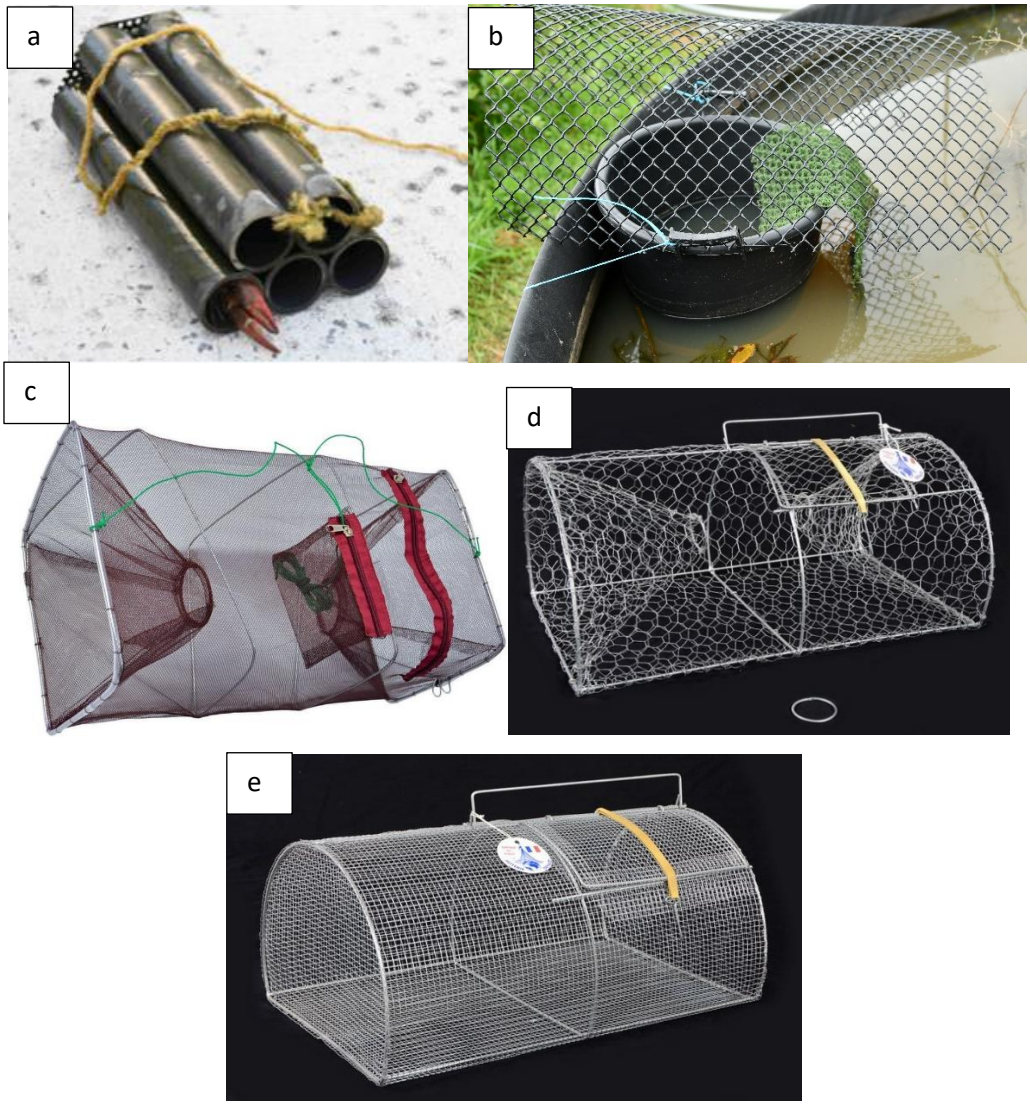

Figure 6: Capture devices. a; artificial refuge trap (ART), b; exit trap, c; Fine mesh trap (FMT), d; course mesh trap (CMT), e; medium mesh trap (MMT). Photo: a and b; Eric Edeline, c; *(tradeinn.com)*, d; *(filets-de-peche.fr)*.

Biometric methods

Biometrics were recorded through a mix of hand used tools and electric measuring boards and scales.

Individuals were placed on a measuring table and the total body length (tip of rostrum to the extremity of the telson) and PIT-tag were recorded. Data was directly communicated through a Bluetooth connection to a an excel macro sheet on a local laptop. Sex (determined from secondary sexual characters, Fig. 2), total body length, body mass, as well as length and width of cephalothorax were recorded for all individuals longer than 19 mm (total length). Additionally, crayfish longer than 55 mm (total length) were measured for the length, height and width of both claws (see Appendix B).

Population analysis

A state-space model is a hierarchical model frequently used in population analysis that can help to understand development over time which cannot be directly observed (Kéry & Schaub, 2011). It is particularly advantageous when investigating systems that include both observed measurements (observed process) and unobserved or "hidden" underlying processes, also known as the states (state process). Therefore, the model can estimate the hidden, but true, sates of a population, and can more accurately represent the underlying prosects that drive the dynamics of the population. The state-space model used in this project was based on the model presented by Kéry & Schaub (2011) and was used as shown below (see Appendix C for model specification).

Observation process:

$$\log(y_{i,t}) \sim \text{Normal}(\log(N_{i,t}), \sigma^2_{i,t}) \qquad \text{(1a)},$$

where i indexes populations (mesocosms), t indexes recapture occasions, $y_{i,t}$ is posterior total population size estimates from the hierarchical spatial CMR model, $N_{i,t}$ is the true (unobserved) population size, and $\sigma^2_{i,t}$ is the posterior variance in $y_{i,t}$ (known from the hierarchical spatial CMR model and here supplied as data).

State process:

$$\begin{gathered} \log(N_{i,t+1}) = \log(N_{i,t}) + r_{i,t} \\ r_{i,t} = r_0 + \beta_1 \overline{Temp} + \beta_2 \overline{\log(N_{i,t})} + \beta_3 \overline{Days} + \varepsilon_i \qquad \text{(1b)}, \\ \varepsilon_i \sim \text{Normal}(0, \sigma^2_\varepsilon) \end{gathered}$$

where $r_{i,t}$ is the growth rate of population i at time t, $\overline{Temp}$ is mean water temperature during transition from t to $t+1$ centered to zero mean, and $\overline{Days}$ is the duration (in days) of transition from t to $t+1$ centered to zero mean.

The model was fitted using Markov Chain Monte Carlo (MCMC) in JAGS 4.3.2 (Plummer, 2003). through the R Statistical Software (v4.3.1; R Core Team, 2023) using the jagsUI R package (Kellner, 2019). r_0 was given a normal prior with mean equal to one and variance equal to 10^3, and β_1, β_2 and β_3 were given a normal prior with zero mean and variance equal to 10^3. The initial population size was given a strong prior with a mean equal to $log(39.9)$ and a variance equal to $log(40.1)$ as the number of introduced crayfish were known (40 in each mesocosm). A total of 3 parallel MCMC chains were run for 20,000 iterations. Every 5th iteration was saved after a burn-in period of 10,000 samples that were removed. A total of 6000 samples were collected from the joint posterior. Parameter convergence was assessed using the Gelman–Rubin statistic (Gelman & Rubin, 1992). The model output, together with trace plots and density plots were used to investigate the results of the model.

Trace plots showed that the chains mixed well and the parameter convergence was good, as confirmed by Rhat values (all <1.003).

Somatic growth analysis

Following Mangel (2006), it is assumed that the rate of change of mass is a balance between anabolic and catabolic factors:

$$\frac{dW}{dt} = anabolic\ factors - catabolic\ factors\ ,$$

and that anabolic factors scale with surface area such that anabolic factors = σL^2, where L is crayfish total length, catabolic factors are a direct result of metabolism and are dependent on body volume such that catabolic factors = cL^3. Together these equations from

$$\frac{dW}{dt} = \sigma L^2 - cL^3 \qquad \text{(2a).}$$

Further assumed, mass scales with length cubed $W(t) = \rho L(t)^3$, where ρ is the body density of the crayfish. After some calculations, Mangel (2006) obtains:

$$\frac{dL}{dt} = \frac{\sigma}{3\rho} - \frac{c}{3\rho} L \qquad \text{(2b)}$$

where $\frac{dL}{dt}$ is the rate of change of the size (here cephalothorax length is used) over a time interval from t to $t+1$, and L is the length of the crayfish at t. Eq. 2b predicts that body length increments $\frac{dL}{dt}$ are a linear function of body length, which intercept is proportional to anabolic scaling parameter sigma, and which slope is proportional to the catabolic scaling parameter c.

The intercept $\frac{\sigma}{3\rho}$ and slope $\frac{c}{3\rho}$ in Eq. 2b above were then estimated, as well as their response to environmental factors, using a linear mixed-effects model:

$$\begin{gathered} \frac{dL_i(t)}{dt} \sim N\left(\mu_i, \sigma_i^2\right) \\ \mu_i = a + bL_i(t) \end{gathered} \qquad \text{(2c),}$$

where i indexes individual crayfish, the growth rate $\frac{dL_i(t)}{dt}$ is normally distributed with the mean μ_i and with the standard deviation σ_i^2, $a = \frac{\sigma}{3\rho}$, and $b = \frac{c}{3\rho}$.

The model is further defined in (2d) and (2e) which attempt to investigate factors that influence anabolism and catabolism in crayfish. They include the effects of sex ($Sex[i]$), population density at time t ($N_i(t)$) estimated from the mean of catch-per-unit effort during the two capture occasions defining time interval «dt», and average temperature ($\bar{T}$) computed as the mean of hourly temperature during the "dt" time interval. Both $N_i(t)$ and $\bar{T}$ were centered to zero mean. These are

independent variables that are defined for both the anabolic processes (2d) and the catabolic processes (2e):

$$a = a_{0,Sex[i]} + a_1 N_i(t) + a_2 \bar{T} + a_j + a_{j,i}$$
$$a_j \sim N\left(0, \sigma^2_{a_j}\right) \quad \text{(2d)}$$
$$a_{j,i} \sim N\left(0, \sigma^2_{a_{j,i}}\right)$$

$$b = b_{0,Sex[i]} + b_1 N_i(t) + b_2 \bar{T} + b_j + b_{j,i}$$
$$b_j \sim N\left(0, \sigma^2_{b_j}\right) \quad \text{(2e).}$$
$$b_{j,i} \sim N\left(0, \sigma^2_{b_{j,i}}\right)$$

The subscript i specifies that the model intends to account for individual-level variability between individuals. Similarly, the j subscript indexes the population (mesocosm) of which the individuals i belong to.

$a_{0,Sex[i]}$ is a fixed effect that captures the effect of sex on crayfish anabolism. a_1 and a_2 are regression slopes (fixed effects) that capture the effects of population density and temperature, respectively, on anabolic processes. $a_j + a_{j,i}$ are normally-distributed, nested random effects that capture individual (i) and group-population-level (j) variability.

A symmetric structure was applied in Eq. 2c, where c_0, $c_1$and c_2 capture the fixed effects of sex, population density and temperature, respectively, on crayfish catabolism, while $c_j$and $c_{j,i}$ are normally-distributed, nested random effects of the individual and population.

The choice of structure of the linear mixed-effects model was based on the hierarchical structure of the data, as well as based on the parsimonious principle, by focusing on a simplistic structure while at the same time effectively explaining the data without being too complex. Further, the model controled for heteroscedastic errors by letting the residual variation (σ_i^2) vary as a power function of individual body length where v and delta are constants to be estimated:

$$\sigma_i^2 = v|L_i(t)|^{\delta} \text{ (2f).}$$

Model 2 was fitted by restricted maximum likelihood (REML) in R using the lme function of the nlme library (Pinheiro et al., 2023). Significant effects of the model parameters were tested in R using ANOVA.

RESULTS

In total, 10996 crayfish were handled during the project. Of these, 2514 were registered as unique PIT-tagged individuals (total body length >55 mm) and 2636 were unique small crayfish (total body length <55 mm).

Population analysis

Posterior estimates from the parameters of the state-space model are shown in Table 2 and Fig. 7.

Table 2: An extract taken from the potential outcome of crayfish population growth estimated from JAGS. The extract shows the posterior estimates of the model output for the following parameters: the intercept of population growth rate (r_0), slope of mean surface water temperature between each occasion (β_1), the slope of population density (β_2), effect of time interval (in days) between primary capture occasions (β_3), and standard deviation of random population effect (ε_i). The model output included lincludes a 95% confidence interval (only mean and standard deviation (sd) is showed here), degree of overlap 0 indicates wether the posterior 95% credible interval includes 0. Rhat is Gelman-Rubin statistic.

Parameter	Mean	sd	Overlaps 0	Rhat
r_0	0.323	0.038	**FALSE**	1.001
β_1	0.197	0.025	**FALSE**	1.000
β_2	0.237	31.688	TRUE	1.002
β_3	0.034	0.002	**FALSE**	1.000
ε_i	0.097	0.036	**FALSE**	1.001

*Statistically significant (overlap = FALSE) effects are in bold.

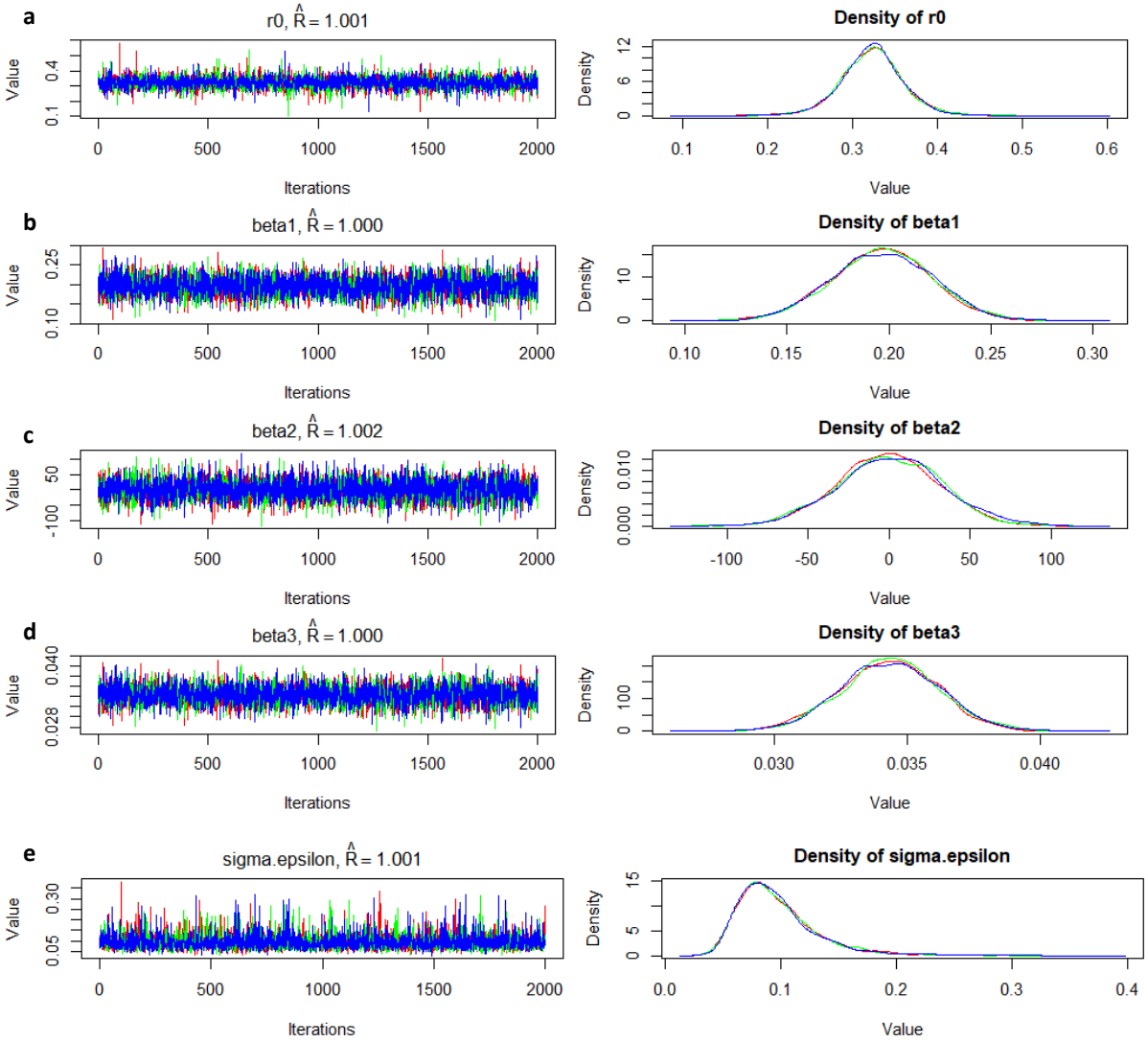

Figure 7: An extract taken from the potential outcome of crayfish population growth rate estimated from JAGS. The extract shows the trace plots and density plots of the following parameters: a; intercept of population growth rate (r_0), b; slope of mean surface water temperature between each occasion (beta1), c; slope of population density (beat2), d; effect of time interval (in days) between each occasion (beta3), e; standard deviation of randosm population effect (sigma.epsilon).

The intercept for crayfish growth rate represents the base line growth of the log-scale population when all other parameters are at their reference level (Table 2, Fig. 7a). On a real scale, mean population growth rate is 1.38 and the population will increase by 38% between two primary capture occasions. No overlap with zero (FALSE) suggests that the population, on average, is unlikely to have no growth, with a 95% confidence.

The next parameter, the slope of temperature effect, represents the effect of mean water temperature on the population growth rate (Table 2, Fig. 7b). The mean estimate of 0.197 indicates that the log of population growth rate increased by 0.197 when temperature increased by one degree

C. One a real scale, the population will increase by 22%, which is a strong effect. Further, the effect of temperature did not overlap with zero (FALSE) and had a small standard deviation (0.025). This positive relationship implies that temperature has a significantly strong positive effect on population growth rate, where higher temperatures are associated with higher growth rates.

The slope of the population density effect on population growth rate assesses the strength of density-dependence in population dynamics (Table 2, Fig. 7c). The posterior of β_2 had high standard deviation (31.688) indicating a very large uncertainty in the effect of density. Additionally, the overlap included zero (TRUE), suggesting that the density had no statistically significant effect on crayfish growth rate overall.

Moving on, the effect of time interval between each primary occasion had an estimate of 0.034, suggesting that the log of population growth rate increased by 0.034 when the time interval increased by one day^{-1} (Table 2, Fig. 7d). It had a small standard deviation (0.002) and did not overlap with zero. The positive relationship indicated that longer time intervals were associated with higher growth rates.

Lastly, the standard deviation of random population effects describes the variation in growth rate among the populations by accounting for population-specific factors not captured by the model predictions (Table 2, Fig. 7e). The estimated mean of 0.097 and the low standard deviation (0.036) suggests that the growth rate of each population deviates a bit and is relatively consistent across all populations.

In addition to investigating the parameters of the state-space model, the posterior distribution for estimated population sizes from the state-space model were projected across all mesocosms and occasions (Fig. 8).

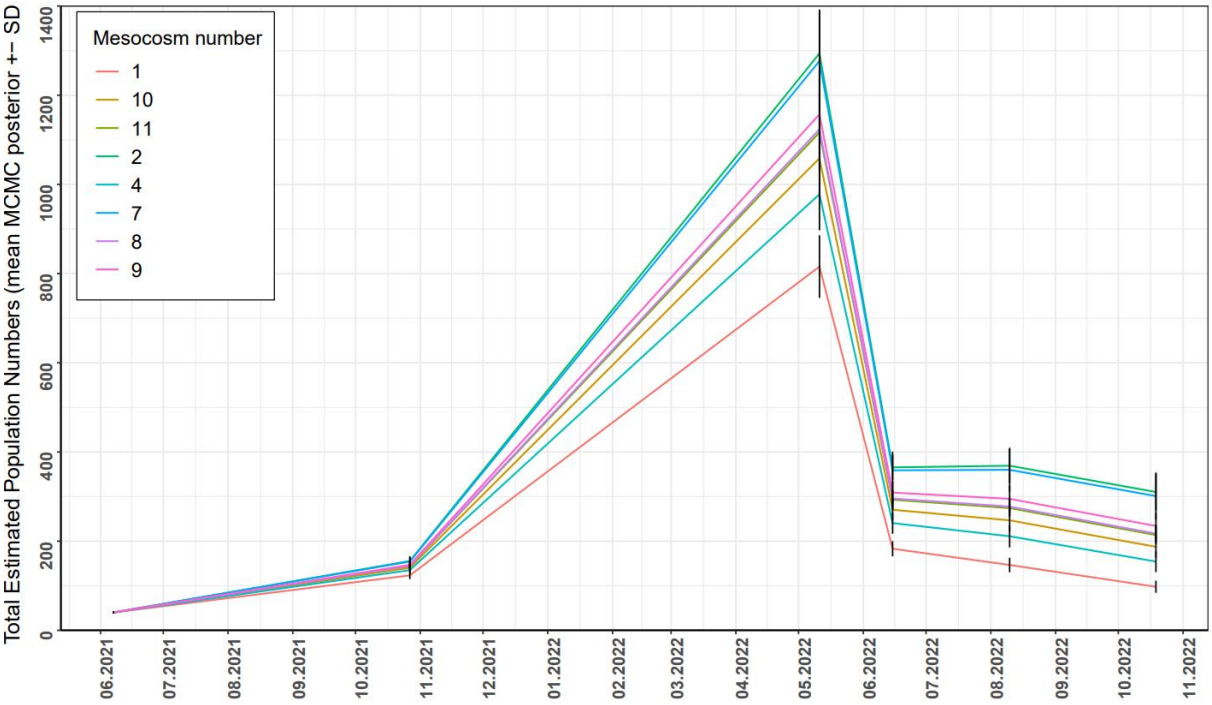

Figure 8: Total estimated crayfish population size (mean MCMC posterior ± SD) in each mesocosm (1, 2, 4, 7, 8, 9, 10, 11) during each primary CMR occasion. See details in Table 2.

These results indicated a consistent pattern for population sizes across all mesocosm and occasions: all mesocosms increased in population size between June 2021 and May 2022, meanwhile almost all mesocosm decreased between May 2022 and October 2022. The two exceptions were mesocosm 2 and 7 which gained +3 and +1 crayfish, respectively, between June and August. This pattern indicates that the main recruitment of new individuals happened during spring, and that there was a clear die-off during the summer. Looking at the overall pattern of the population sizes across all mesocosm and occasions, the state-space model suggested a small increase in population sizes from introduction in June 2021 to the first capture occasion in October 2021 (interval of mean; 123.3– 155.4, interval of sd; 8.2-10.6). The biggest population sizes were estimated in May 2022 (interval of mean; 815.7-1293.7, interval for sd; 70.0-114.7), meanwhile the most prominent decrease in population size was estimated between May and June 2022 (interval of mean;183.0-367.5, interval for sd;16.8-41.2). From June 2022, a small decrease was estimated in August 2022 (interval of mean;146.6-369.1, interval for sd;16.0-49.2), and from August to October 2022 (interval of mean; 97.8-310.2, interval for sd;13.5-52.8).

Somatic growth analysis

The results of the linear mixed-effects model revealed that sex, population density, temperature, and individual size had significant effects on crayfish body-size increments (Table 3). The estimated intercept of crayfish body-size increments represents the base line increments when all other

variables are at their reference level. It indicated that when these conditions were met, the average growth rate of a crayfish were 0.11471 mm/day ($p<0.001$). The effect of being male on the anabolic rate showed that, on average, males grow faster than females by 0.06819 mm/day ($p<0.001$). On the other hand, a one-unit increase in crayfish density (cpue) was associated with a decrease in the anabolic rate by -0.00093 mm/day ($p<0.001$), indicating a negative association between population density and food intake rate and/or energy allocation to stomatic growth. In contrast, a one degree C increase in temperature was associated with an increase in growth rate by 0.00679 mm/day ($p<0.001$). Lastly, the effect of cephalothorax length represents how growth rate changes with individual sizes. The estimate -0.00210 mm/day ($p<0.001$) indicated that the growth rate decreased with individual size.

Table 3: Parameter estimates for the fixed effects of the linear-mixed effects model. The results indicate the effects of the parameters sex.M (males), population density (mean cpue), mean hourly temperature during the "dt" time interval (se Eq. 2a) (Temperature), and cephalothorax length (mm) on somatic growth rate. Additionally, it shows the interaction effects between sex and cephalothorax length, between cpue and cephalothorax length, and between temperature. The model output includes the variables, their estimated coefficients (value), standard deviation, degrees of freedom (DF), t-vales and p-values. All p-values < 0.05 were considered significant.

Variables	Value	Std. error	DF	t-value	p-value*
Intercept	0.11471	0.00871	1098	13.16377	**<0.001**
Sex.M	0.06819	0.01224	461	5.57235	**<0.001**
Mean cpue	-0.00093	0.00021	461	-4.42921	**<0.001**
Temperature	0.00679	0.00240	461	2.83260	**<0.005**
Cephalothorax length	-0.00210	0.00021	461	-10.25010	**<0.001**
Sex.M: Cephalothorax length	-0.00167	0.00030	461	-5.50552	**<0.001**
Mean cpue: Cephalothorax length	0.00002	0.00001	461	3.23345	**0.001**
Temperature: Cephalothorax length	-0.00070	0.00005	461	-3.35965	**<0.001**

*Statistically significant ($p<0.05$) effects are in bold.

The random effects estimated a standard deviation of the random intercepts of mesocosm to be 0.00556, indicating a low variation within the intercept, and thereby anabolism, between mesocosm. Further, the estimated standard deviation of the random intercepts of the combination of unique crayfish identities nested within mesocosm was approximately 0.00061. This suggests a lower variation between individuals within the same mesocosm. Finally, the variance function of

cephalothorax length had an estimated power of -0.39738, indicating a strong negative relationship where the residual variability decreases when cephalothorax length increases.

The last part of the crayfish growth model investigated sex-cephalothorax length, population density-cephalothorax length, and temperature-cephalothorax length interactions on crayfish somatic growth rate (Table 3). Significant interaction effects were observed for all of them (all p-values<0.001). The interaction effects of sex suggest that the male body growth slows down with increasing cephalothorax length faster than the female body growth, suggesting that the males have a higher catabolic rate (energy loss rate).

Interaction plots showed that the cpue-by-cephalothorax length interaction reflected a selective decrease in growth rate of small crayfish under high crayfish density (Fig. 9). As the crayfish became larger their growth rate decreased where eventually the largest crayfish stopped growing (length increments = 0). This occurred at all densities. Additionally, the plot indicated a higher intercept and a steeper slope at lower densities, suggesting that both anabolic rate and catabolic rate decreased as population density increased.

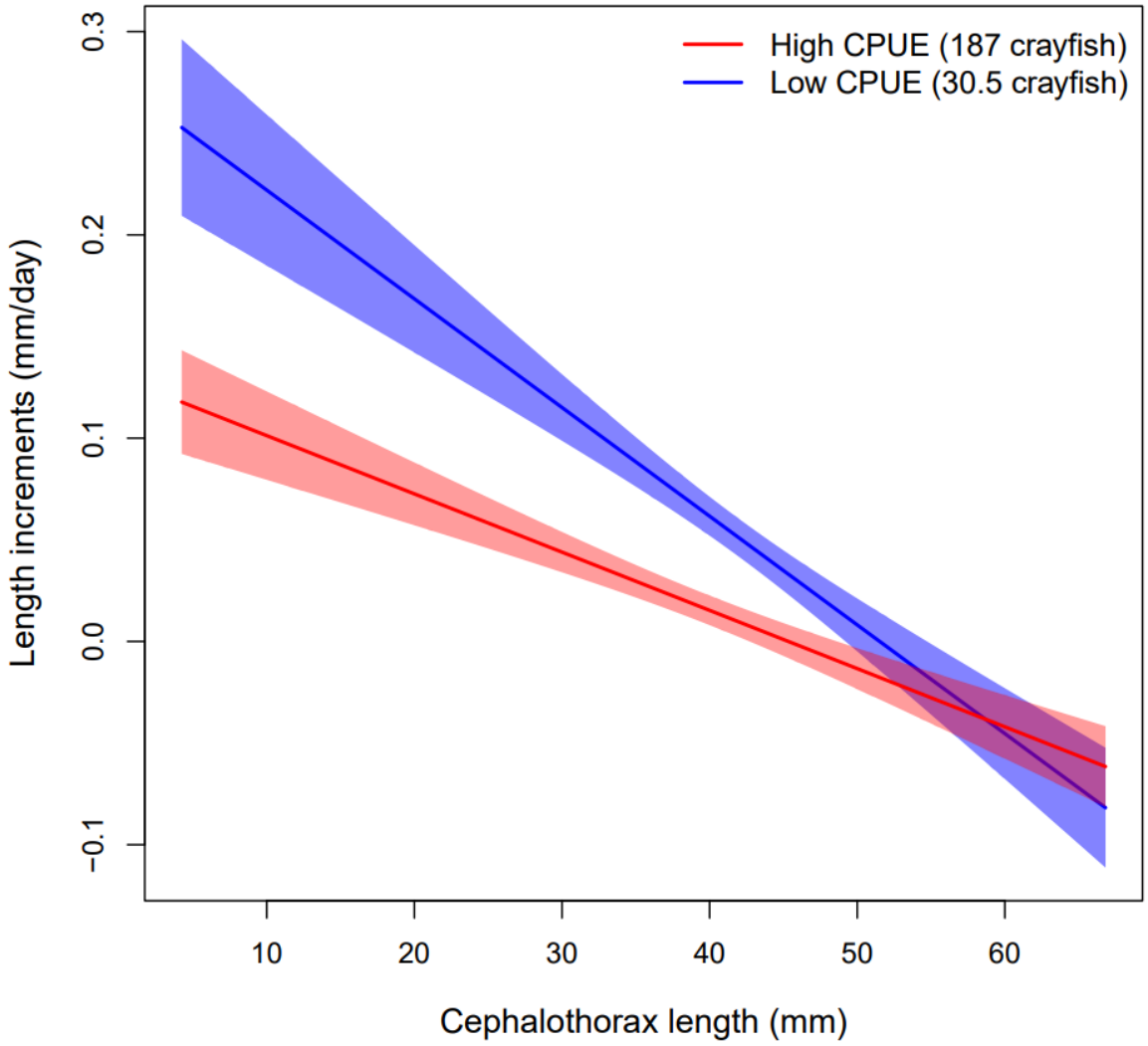

Figure 9: Interaction plot representing the interaction effects between cephalothorax length (mm) and mean cpue on bodily growth rate for males. Each line shows different levels of centered cpue (centered to zero) indicated by color; high cpue (187 crayfish)(red), and low cpue (30.5 crayfish)(blue). Predicted values ware based on a linear mixed-effects model (Eq. 2) with associated confidence intervals (shaded regions on each line) on the predictions.

The interaction plot of temperature-cephalothorax length interaction also displayed a strong interaction on crayfish stomatic growth rate. The somatic growth rate decreased as the crayfish grew larger for all temperatures (Fig. 10). Further, a higher intercept and a steeper slope was estimated for higher temperatures. This indicated that both the anabolic rate and catabolic rate increased as temperature increased.

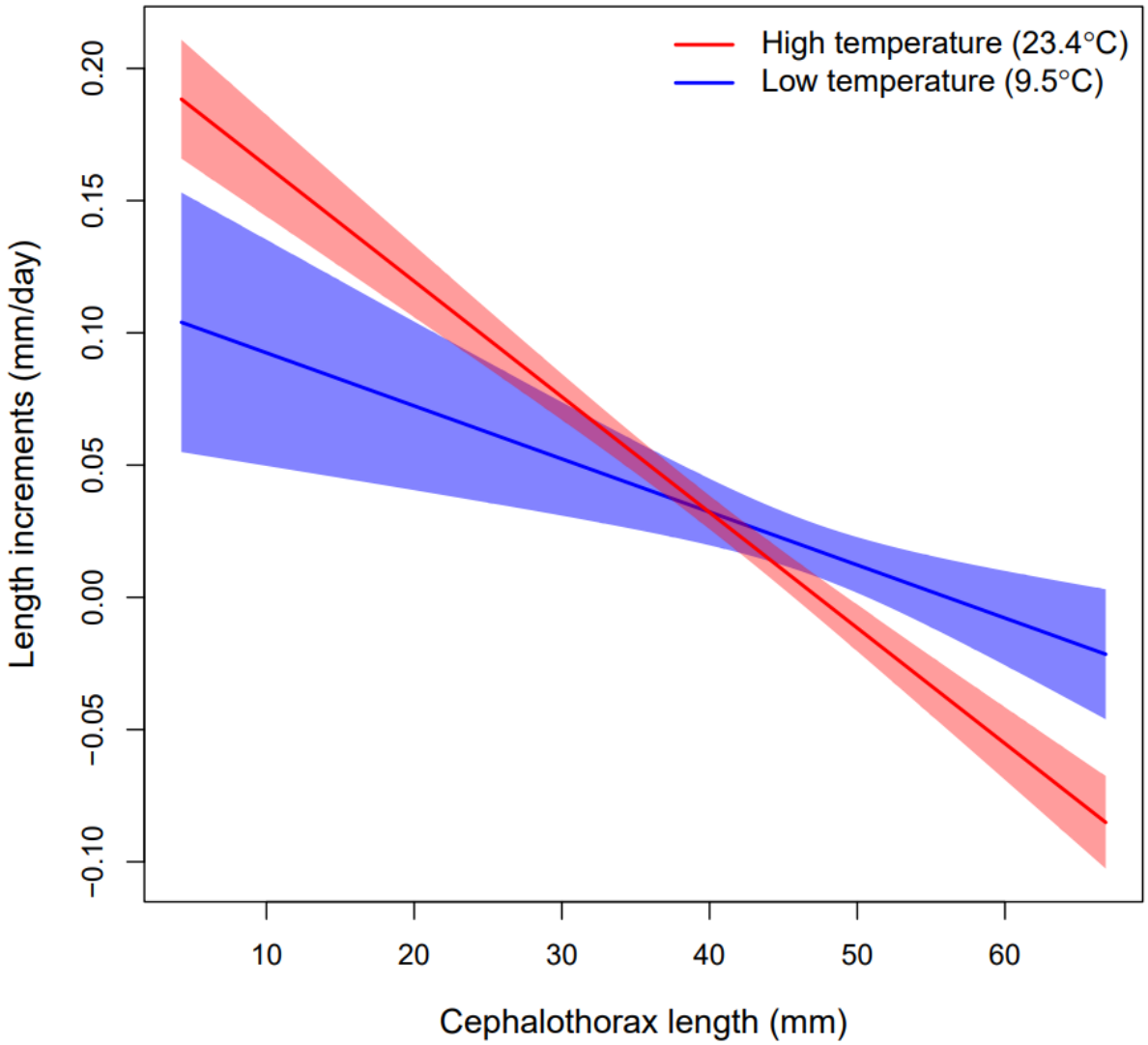

Figure 10: Interaction plot representing the interaction effects between cephalothorax length (mm) and temperature (mean hourly temperature between two sampling occasions) on bodily growth rate for males. Each line shows different levels of centered temperature (centered to zero) indicated by color; high temperature (23.4°C)(red), and low temperature (9.5°C)(blue). Predicted values ware based on a linear mixed-effects model (Eq. 2) with confidence intervals (shaded regions on each line) on the predictions.

DISCUSSION

Population dynamics

This project looked at how different environmental factors affect the overall mean population growth rate of *P. clarkii,* where temperature and density were in focus.

The temperature was estimated to have a significant effect on the overall mean population growth rate where higher temperatures led to it increasing (Tabel 2). It is not surprising that this occurred,

considering the seasonal activity and circadian rhythm of *P. clarkii.* It is well known that crustaceans exhibit these activities under the influence of ecological and physiological mechanisms, where ecological factors are commonly related to temperature, photoperiod, competition and resource availability (Brown, 1961; Capelli & Hamilton, 1984; Correia, 1998; Somers & Stechey, 1986). Additionally, temperature is positively correlated with light, where light is a major environmental que to trigger physiological processes like reproduction, and by increasing day length (photoperiod) alongside temperature reproductive abilities have been shown to be enhanced in *P. clarkii* (Daniels et al., 1994; Liu et al., 2013). Increased activity and reproduction can lead to an increased population growth. Therefore, the effect of temperature on population growth rate is suggested to follow seasonality, where higher longer photo periods and simultaneously higher temperatures enhance the reproduction, thus increasing the population growth.

In contrast, the population density was estimated to have no significant effect on the overall mean population growth rate (Table 2). This is unexpected given that density dependence is a well-known phenomenon where population growth rate tends to decrease as density increases. This is because higher competition for resources, shelter and mates is positively associated with higher mortality and lower birth rate, thus resulting in reduced population growth rate. Despite the lack of statistical significance in the model, the estimated population size and the scarce resource availability suggest otherwise (Fig. 8). Seeing how the estimated population size underwent a substantial decrease from May 2022 (mean: 815.7-1293.7) to June 2022 (mean: 183.0-365.5) across all mesocosm, accompanied by all plants being mostly gone by May 2022 across all mesocosms, this is likely to be a result of increased competition for space and resources. Thereby, this provides a compelling ecological basis supporting the proposal of a strong negative density-dependence precent in the mesocosms. Yet again, looking at the estimated effect of density, the standard deviation was substantially large (31.688) indicating a large uncertainty in the effect of density. This was likely due to the length of the time series being too short for the model to robustly estimate its strength. By increasing the length and frequency of the CMR sessions, it could provide a better foundation for the model to estimate the significance of density effect on population growth rate.

The estimated mean population sizes across mesocosms and primary occasions gave an opportunity to speculate on how the population growth progressed throughout the project (Fig. 8). The general pattern of variation in estimated population size suggested a high increase in population size during spring 2022, and a large die-off during transition from spring to summer, where it slowly decreased through summer and into autumn. All standard deviations were regarded as small in relation to their associated population size, and therefore deemed trustworthy. Only two mesocosms (two and seven

in August 2022) deviated from this concurrent pattern, as they had a standard deviation more than twice the size of the other mesocosms and were deemed untrustworthy.

The large differences between the population size in May 2022 and June 2022 was most likely due to high competition and scares resource availability. When the crayfish were first introduced to the mesocosms, the living conditions were quite good with clean water, available plants and insects to eat, and few crayfish to compete with. In October 2021, females bearing juveniles were observed. As temperature and daylight increased during spring there was most likely a large recruitment in this period, leading to a high population size in May. Transitioning to the very small, estimated population size in June 2022, it is suggested that a large amount of the crayfish died within this short period of one month, most likely due to the populations exceeding their carrying capacity. *P. clarkii* have been shown to increase its foraging activity during spring and summer, meanwhile decrease it during winter (Correia, 1998). This could explain why all plants and insects were observed to be mostly gone by May, subsequently decrease the water quality by restricting the oxygen production, leading the water to "rot". The combination of isolation (not able to venture to new habitats), higher competition, and very low food availability resulted in a large die-off. It is also speculated that these poor living conditions promoted cannibalism on weak (molting) and small crayfish, however this was not possible to be confirmed.

Moving on to late summer and September 2022, the water in most of the mesocosm was murky and ill-smelling. Additionally, some large crayfish were observed at the water surface thought to be gasping for air, as well as a few dead floating at the surface. This might provide insight into why the estimated population size kept on shrinking throughout summer and autumn of 2022. It should be emphasized once again that these are only speculations. Incorporating analysis on survival data would provide a more precise insight and is recommended for future studies which aim to better understand population dynamics within earlier phases of crayfish invasion.

Somatic growth

The fixed effects analysis revealed that temperature, population density, sex and crayfish length had a significant effect on the somatic growth rate of crayfish (Table 3). They will each be addressed here in this order.

Effects of temperature on somatic growth rate

First, temperature had a positive relationship with somatic growth rate and indicated increased anabolic rate with increased temperature (Table 3). This is expected, given that increased temperatures are well known for influencing and accelerating biochemical processes, thus making more energy available for growth-related processes. Crayfish are ectothermic organisms, meaning

that their body temperature is influenced by their surrounding environment. Under constant energy intake, warmer temperatures will increase somatic growth only if anabolism increases faster with temperature than catabolism. Thereby, warmer temperatures can enhance metabolic rates and increase anabolic processes, thus increasing individual growth rate, meanwhile cold temperatures can slow them down and result in a slower growth rate. The interaction plot of temperature-cephalothorax length indicated that for higher temperatures both anabolic rate and catabolic rate increased (Fig. 10). Higher temperatures require higher cellular kinetic energy, and will directly increase the resting metabolic rate (the use of energy needed to maintain basic body functions while resting) of an organism (Gillooly et al., 2001). Elevated metabolic rates of both anabolic and catabolic processes imply that more energy from nutrient intake is allocated toward growth, and as long as the crayfish stays within temperatures of optimal growth conditions, the catabolic rate will not exceed the anabolic rate, allowing the organism to grow faster.

P. clarkii has a preferred temperature range of 21.8C°-26.9C° (Tattersall et al., 2012), a tolerance levels of maximum 35C° (J. V. Huner & Barr, 1991), and its range of optimal growth was 22C°-30C° (J. Huner, 1988). These species-specific temperatures align with the monthly range of surface water temperatures during spring and summer (Fig. 5). Crayfish living in optimal somatic growth conditions could result in more crayfish maturing faster and being recruited into the population. As a result, an increase in somatic growth rate could increase the population growth rate and therefore explain the large increase in population size in May 2022 (Fig. 8). Following this logic, the population size would be expected to increase throughout the summer of 2022, however looking at the estimated population size, this was not the case. This will be explained by addressing density effects on somatic growth rate.

Effects of population density on somatic growth rate

Similar to temperature, the effects of density was expected. As density increased, the anabolic rate decreased, suggesting that higher densities resulted in crayfish allocating energy less towards somatic growth rate (Table 3). This makes sense, as there is more competition for resources at higher densities, and when resource availability becomes scares very little nutrition is available and would result in the catabolic rate exceeding the anabolic rate, thereby decreasing the somatic growth rate. Seeing that density had an impact on individual growth rate, it could support the proposal of density effecting population growth despite the results of the model. As somatic growth is being suppressed at higher density, it is logical that the rate of reaching maturity also would slow down. This could also lower the number of new recruits to the population, thus also decreasing the population growth rate. Seeing that density had a strong impact on individual growth rate, it also supports the proposal of density effecting population growth despite the results of the model.

As for the interaction plot of cpue-cephalothorac length, it was suggested that both anabolic rate and catabolic rate decreased at higher densities (Fig. 9). Again, higher densities entail higher competition and more risk-taking. A study by Schirf et al. (1987) showed that food deprivation gave significant decrease in muscle of *P. clarkii*, making it weaker in aggressive encounters and are more prone to loos and be eaten (cannibalism). This is especially true for smaller crayfish due to the aggressive and hierarchical nature of crayfish, as several studies have shown that smaller crayfish are ranked lower in the hierarchy and loos easier against bigger crayfish when competing for food and shelter (Alonso & Martínez, 2006; Edsman & Jonsson, 1996; Figler et al., 1999; Nakata & Goshima, 2003; Ranta & Lindström, 1992, 1993). Small crayfish were also suggested to have a lower somatic growth at high densities (Fig. 9), which seems to agree with these studies. Taking this into consideration, it builds up under the speculation of cannibalism being a partly cause to the large die-off in June 2022, as mentioned earlier in the discussion. Unfortunately, the State-space model did not allow to capture the effect of different crayfish size, so this will remain as an object of conjecture. It is therefore recommended for future studies utilize size-class structured state-space model to provide a different perspective.

Sexual differences in body growth rate

The males were shown to have a higher growth rate than females (higher anabolic rate), and respectively a faster loss of energy (higher catabolic rate) (Table 3). Crayfish are known to establish hierarchy, and when necessary resources are limited, such as food, space, shelter and mates, agonistic behavior tend to increase among social animals (Wilson, 1975). Crustaceans are well known for establishing social dominance hierarchies to maintain non-aggressive access to these resources (Edwards et al., 2005). A study by Wang et al. (2011) showed that males are heavier and have longer and wider chelae compared to females of same body length, and this makes the males more aggressive and better fit for competition. This has also been shown for other crayfish species (Rodger & Starks, 2020). These results suggest that sexual dimorphism plays a role in the energy allocation of crayfish, where males allocate more energy towards body growth as this gives them an upper hand in competition, meanwhile females are more stable in their energy spending and focus it more towards brooding of eggs and juveniles. Therefor it is natural that the males have a higher anabolic rate and catabolic rate than females.

Effects of cephalothorax length on somatic growth rate

Mangle's growth model, which this project's individual growth model was based on, captures the relationship between the individual growth rate and the size (here cephalothorax length is used) of the crayfish. Its assumptions of a strictly negative growth~length relationship aligned with the results of this project, where somatic growth rate was estimated to decrease as the crayfish grew larger

(Tabel 2, Fig.9,10). This was consistent across all temperatures and densities. Additional, variability in the random effects decreased as cephalothorax length increased (residual sd = -0.39738). Meaning, that larger crayfish tend to exhibit a more consistent somatic growth rate across different mesocosms. It is noteworthy that Mangel's model is based on the principles of von Bertalanffy's theory (1934) of individual growth. This theory has laid the foundation for modeling growth trajectories across multiple organisms and is rooted in the fundamental principle of negative allometric growth. Therefore, it is widely used for organisms that exhibit reduced growth rate as they approach their maximum size. As organisms grow larger and become more mature, more resources are allocated towards vital processes such as reproduction, resulting in a decreased growth rate. Again, the results of the project aligned with these principles across all temperatures and densities of this project.

However, what did differ from the Mangle's model was the type of biological effect density had on somatic growth rate. As mentioned earlier, Mangle's model assumes a negative growth~length relationship which is mainly determined by physiological factors, specifically catabolic processes. In contrast to this, the cpue-cephalothorax length interaction suggested selective decrease in the somatic growth rate of small crayfish under high crayfish densities, thus not a catabolic effect, but rather an ecological effect. This suggests that in this project, ecology may have a stronger effect on somatic growth than physiology. Considering the hierarchical nature of crayfish, this makes sense. As mentioned earlier, smaller crayfish are more likely to lose in competition for food and shelters with larger individuals. At higher densities with scarce resources, smaller crayfish are more likely to encounter other crayfish as they compete for food, thereby putting them in a bigger disadvantage. This means that ecological factors like density seems to have a large impact on the somatic growth of the smaller crayfish.

CONCLUTION

P. clarkii is well known for being a successful invader worldwide and is a quite well studied species. Despite this, little is known of what happens to the population during invasion, and especially during the earlier phases of establishments. This project has focused on estimating the effects of a handful of ecological and physiological factors that influence the population dynamics and individual somatic growth of *P. clarkii* in replicated self-sustained mesocosms.

First, temperature was found to have a significant effect on population growth rate, meanwhile population density did not. It was theorized that seasonality and circadian rhythm were the drivers for simultaneous increase of light and temperature during spring, which promoted reproduction and thereby increases the population growth rate. Further, it was proposed that the model was unable to capture the strength of the density effects due to the short time series of sampling. This was backed

up by the patterns of the estimated population sizes, alongside the significant influence of density on somatic growth rate, having a possible ripple effect on the dynamics of population growth rate.

The estimated population size across mesocosm and primary occasions were used to speculate on how the population growth progressed throughout the project. The high population size during spring 2022 was thought to be mainly driven by the good living conditions (low competition, good food availability) which led to high recruitment. Due to the high competition and food deprivation in late spring and summer 2022, it was further speculated that the population had reached its bearing capacity leading to a large die-off in summer 2022.

As for the individual growth analysis, it was revealed that population density, temperature, sex and individual cephalothorax length had a significant effect on somatic growth rate. The effects of density and temperature were both as expected, where higher temperatures promoted somatic growth rate, meanwhile higher densities reduced somatic growth rate. Further, both sex and crayfish size seamed to play a role in energy allocation, due to the hierarchical nature of *P. clarkii.* It was suggested that ecology may have a stronger effect on somatic growth than physiology, due lower somatic growth rate in small crayfish at higher densities.

The state-space model served as a valuable tool shedding light on the invasive species' population dynamics in the earlier stages of establishment, meanwhile the findings guided by the refined model of Mangle have contributed to insight to crayfish somatic growth dynamic. Looking at how all the populations crashed in the end of the project and how they continued to decline in population size, it is most likely that they will not succeed in establishing an invasion. However, due to the short time span of the project, no defined conclusion can be drowned. Therefore, much remain to be investigated. This thesis has hopefully laid a foundation for future studies to build upon and develop more insight into the earlier phases of establishment of the invasive crayfish *P. clarkii*.

REFERENCES

Alonso, F., & Martínez, R. (2006). SHELTER COMPETITION BETWEEN TWO INVASIVE CRAYFISH SPECIES: A LABORATORY STUDY. *Bulletin Français de La Pêche et de La Pisciculture*, *380–381*, Artikkel 380–381. https://doi.org/10.1051/kmae:2006015

Brown, F. A. (1961). Diurnal Rhythm in Cave Crayfish. *Nature*, *191*(4791), Artikkel 4791. https://doi.org/10.1038/191929b0

Capelli, G. M., & Hamilton, P. A. (1984). Effects of Food and Shelter on Aggressive Activity in the Crayfish Orconectes rusticus (Girard). *Journal of Crustacean Biology*, *4*(2), 252–260. https://doi.org/10.2307/1548022

Correia, A. M. (1998). Seasonal and Circadian Foraging Activity of Procambarus clarkii (Decapoda, Cambaridae) in Portugal. *Crustaceana*, *71*(2), 158–166.

Crooks, J. A., & Rilov, G. (2009). The Establishment of Invasive Species. I G. Rilov & J. A. Crooks (Red.), *Biological Invasions in Marine Ecosystems: Ecological, Management, and Geographic Perspectives* (s. 173–175). Springer Berlin Heidelberg. https://doi.org/10.1007/978-3-540-79236-9_9

Daniels, W., Dabramo, L., & Graves, K. (1994). Ovarian Development of Female Red Swamp Crayfish (procambarus-Clarkii) as Influenced by Temperature and Photoperiod. *JOURNAL OF CRUSTACEAN BIOLOGY*, *14*(3), 530–537. https://doi.org/10.2307/1548999

Doherty, T. S., Glen, A. S., Nimmo, D. G., Ritchie, E. G., & Dickman, C. R. (2016). Invasive predators and global biodiversity loss. *Proceedings of the National Academy of Sciences*, *113*(40), 11261–11265.

Edsman, L., & Jonsson, A. (1996). The effects of size, antennal injury, ownership, and ownership duration on fighting success in male signal crayfish, Pacifastacus leniusculus (Dana). *Nordic Journal of Freshwater Research (Sweden)*.

Edwards, D. H., Herberholz, J., & Nelson, R. (2005). Crustacean models of aggression. *The biology of aggression*, 38–61.

Figler, M. H., Cheverton, H. M., & Blank, G. S. (1999). Shelter competition in juvenile red swamp crayfish (Procambarus clarkii): The influences of sex differences, relative size, and prior residence. *Aquaculture*, *178*(1), 63–75. https://doi.org/10.1016/S0044-8486(99)00114-3

Galib, S. M., Sun, J., Gröcke, D. R., & Lucas, M. C. (2022). Ecosystem effects of invasive crayfish increase with crayfish density. *Freshwater Biology*, *67*(6), 1005–1019. https://doi.org/10.1111/fwb.13897

Gelman, A., & Rubin, D. B. (1992). Inference from iterative simulation using multiple sequences. *Statist. Sci.*, *4*, 457–472. https://doi.org/10.1214/ss/1177011136

Gherardi, F. (2006). Crayfish invading Europe: The case study of Procambarus clarkii. *Marine and Freshwater Behaviour and Physiology*, *39*(3), 175–191. https://doi.org/10.1080/10236240600869702

Gherardi, F. (2007). *Biological invaders in inland waters: Profiles, distribution, and threats* (Bd. 2). Springer.

Gillooly, J. F., Brown, J. H., West, G. B., Savage, V. M., & Charnov, E. L. (2001). Effects of Size and Temperature on Metabolic Rate. *Science*, *293*(5538), 2248–2251. https://doi.org/10.1126/science.1061967

Girard, C. F. (1852). A revision of the North American Astaci, with observations on their habits and geographic distribution. *Proceedings of Academy of Natural Sciences of Philadelphia*, 6:87-91.

Global Invasive Species Database. (2023). http://www.iucngisd.org/gisd/speciesname/Procambarus+clarkii

Havel, J. E., Kovalenko, K. E., Thomaz, S. M., Amalfitano, S., & Kats, L. B. (2015). Aquatic invasive species: Challenges for the future. *Hydrobiologia*, *750*, 147–170.

Hobbs, J., & Horton, H. (1974). *Synopsis of the families and genera of crayfishes (Cruatacea: Decapoda)*.

Holdich, D. (1988). The dangers of introducing alien animals with particular references to crayfish. *Freshwater crayfish*, *7*, 15–30.

Holdich, D. M. & Sibley, P. J. (eds) (2003). Management & Conservation of Crayfish. Proceedings of a conference held on 7th November, 2002. Environment Agency, Bristol. 217 pp.

Huner, J. (1988). Procambarus in North America and elsewhere. *Freshwater crayfish: biology, management and exploitation.*, 239–261.

Huner, J. (2018). *Freshwater Crayfish Aquaculture in North America, Europe, and Australia: Families Astacidae, Cambaridae, and Parastacidae*. CRC Press.

Huner, J. V., & Barr, J. (1991). *Red swamp crawfish: Biology and exploitation*.

Jones, J. P. G., Rasamy, J. R., Harvey, A., Toon, A., Oidtmann, B., Randrianarison, M. H., Raminosoa, N., & Ravoahangimalala, O. R. (2009). The perfect invader: A parthenogenic crayfish poses a new threat

to Madagascar's freshwater biodiversity. *Biological Invasions*, *11*(6), 1475–1482. https://doi.org/10.1007/s10530-008-9334-y

Keller, R. P., Geist, J., Jeschke, J. M., & Kühn, I. (2011). Invasive species in Europe: Ecology, status, and policy. *Environmental Sciences Europe*, *23*, 1–17.

Kellner, K. (2019). JagsUI: a wrapper around "rjags" to streamline "JAGS" analyses. https://CRAN.R-project.org/package=jagsUI

Kéry, M., & Schaub, M. (2011). *Bayesian Population Analysis using WinBUGS: A Hierarchical Perspective*. Academic Press.

Liu, S., Gong, S., Li, J., & Huang, W. (2013). Effects of Water Temperature, Photoperiod, Eyestalk Ablation, and Non-Hormonal Treatments on Spawning of Ovary-Mature Red Swamp Crayfish. *NORTH AMERICAN JOURNAL OF AQUACULTURE*, *75*(2), 228–234. https://doi.org/10.1080/15222055.2012.746247

Longshaw, M., & Stebbing, P. (2016). *Biology and ecology of crayfish*. CRC Press.

Loureiro, T. G., Anastácio, P. M. S. G., Araujo, P. B., Souty-Grosset, C., & Almerão, M. P. (2015). Red swamp crayfish: Biology, ecology and invasion-an overview. *Nauplius*, *23*, 1–19.

Mangel, M. (2006). *The theoretical biologist's toolbox: Quantitative methods for ecology and evolutionary biology*. Cambridge University Press.

Molnar, J. L., Gamboa, R. L., Revenga, C., & Spalding, M. D. (2008). Assessing the global threat of invasive species to marine biodiversity. *Frontiers in Ecology and the Environment*, *6*(9), 485–492.

Nakata, K., & Goshima, S. (2003). Competition for Shelter of Preferred Sizes between the Native Crayfish Species Cambaroides Japonicus and the Alien Crayfish Species Pacifastacus Leniusculus in Japan in Relation to Prior Residence, Sex Difference, and Body Size. *Journal of Crustacean Biology*, *23*(4), 897–907. https://doi.org/10.1651/C-2411

NISIC. (2023, mai 17). https://www.invasivespeciesinfo.gov/what-are-invasive-species

Penn, G. H. (1943). A Study of the Life History of the Louisiana Red-Crawfish, Cambarus Clarkii Girard. *Ecology*, *24*(1), 1–18. https://doi.org/10.2307/1929856

Pinheiro, J. C., Bates, D. M., & R Core Team. (2023). *nlme: Linear and Nonlinear Mixed Effects Models* (R package version 3.1-162). https://CRAN.R-project.org/package=nlme

Plummer, M. (2003). *JAGS: a program for analysis of Bayesian graphical models using Gibbs sampling*. Proceedings of the 3rd international workshop on distributed statistical computing, Vienna, Austria.

R Core Team. (2023). *R: A Language and Environment for Statistical Computing*. R Foundation for Statistical Computing. https://www.R-project.org/

Ranta, E., & Lindström, K. (1992). Power to Hold Sheltering Burrows by Juveniles of the Signal Crayfish, Pasifastacus leniusculus. *Ethology*, *92*(3), 217–226. https://doi.org/10.1111/j.1439-0310.1992.tb00961.x

Ranta, E., & Lindström, K. (1993). *Body size and shelter possession in mature signal crayfish, Pacifastacus leniusculus*. 125–132.

Rodger, A. W., & Starks, T. A. (2020). Length–Weight and Morphological Relationships for Ecological Studies Involving Ringed Crayfish (Faxonius neglectus neglectus): An Extraregional Invader. *Southeastern Naturalist*, *19*(4), 637–648. https://doi.org/10.1656/058.019.0403

Royle, J. A., & Converse, S. J. (2014). Hierarchical spatial capture–recapture models: Modelling population density in stratified populations. *Methods in Ecology and Evolution*, *5*(1), 37–43.

Rutledge, K., McDaniel, M., Teng, S., Hall, H., & Ramroop, T. (2022, september 27). *Invasive Speceis* [Encyclopedic entry]. National Geographic. https://education.nationalgeographic.org/resource/invasive-species

Schirf, V. R., Turner, P., Selby, L., Hannapel, C., de la Cruz, P., & Dehn, P. F. (1987). Nutritional status and energy metabolism of crayfish (Procambarus clarkii, Girard) muscle and hepatopancreas. *Comparative Biochemistry and Physiology A, Comparative Physiology*, *88*(3), 383–386. https://doi.org/10.1016/0300-9629(87)90050-8

Somers, K. M., & Stechey, D. P. M. (1986). Variable Trappability of Crayfish Associated with Bait Type, Water Temperature and Lunar Phase. *The American Midland Naturalist*, *116*(1), 36–44. https://doi.org/10.2307/2425935

Tattersall, G. J., Luebbert, J. P., LePine, O. K., Ormerod, K. G., & Mercier, A. J. (2012). Thermal games in crayfish depend on establishment of social hierarchies. *Journal of Experimental Biology*, *215*(11), 1892–1904. https://doi.org/10.1242/jeb.065946

von Bertalanffy, L. (1934). Untersuchungen Über Die Gesetzlichkeit Des Wachstums: I. Teil: Allgemeine Grundlagen Der Theorie; Mathematische Und Physiologische Gesetzlichkeiten Des Wachstums Bei Wassertieren. *Wilhelm Roux'Archiv für Entwicklungsmechanik der Organismen*, *131*, 613–652.

Wang, Q., Yang, J. X., Zhou, G. Q., Zhu, Y. A., & Shan, H. (2011). Length–weight and chelae length–width relationships of the crayfish Procambarus clarkii under culture conditions. *Journal of Freshwater Ecology*, *26*(2), 287–294. https://doi.org/10.1080/02705060.2011.564380

Williams, B. K., Nichols, J. D., & Conroy, M. J. (2002). *Analysis and Management of Animal Populations*. Academic Press.

Wilson, E. (1975). *Sociobiology: The New Synthesis Harvard University Press Cambridge*.

APPENDIX A - Marking of crayfish

Placement of PIT-tags:

The photo shows a large crayfish (total body length > 55 mm) with a correctly inserted PIT-tag into the muscle of the left part of the 3rd abdominal segment.

Marking with nail polish:

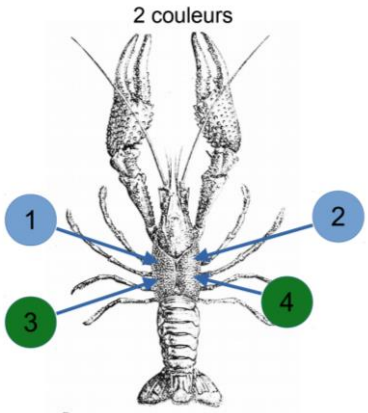

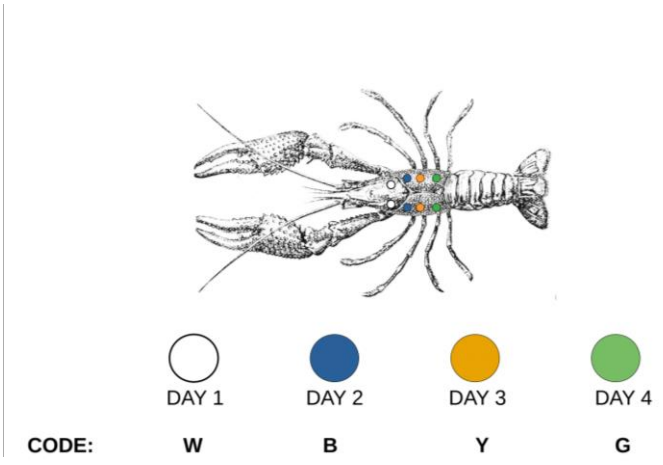

The photos show the order of when each color was used (day 1; white, day 2; blue, day 3; orange, day 4; green), and how to place each color dot on the cephalothorax of the crayfish. No color was used on the last day as this was the last day of the sampling period.

RULES TO MEASURING CRAYFISH AND RECORDING MEASUREMENT DATA

Eric Edeline 03/08/2022

TOTAL LENGTH AND CEPHALOTHORAX LENGTH

Total length is taken using the measuring board from the tip of the rostrum to the end of the telson (Fig. 1). Cephalothorax length and width (Fig. 1) are measured using digital calipers.

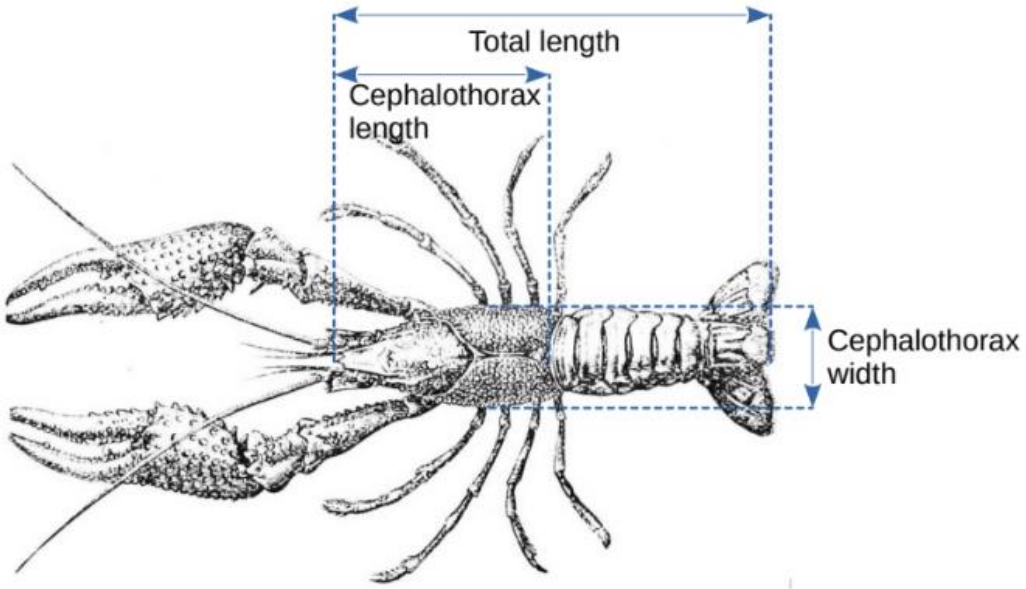

Fig. 1. Position of total and cephalothorax length measurements on *P. clarkii*.

If the rostrum is broken, see below.

CHELA MEASUREMENTS
(Chela length, width and height)

Chela length should be measured from the base of joint to the tip of non-mobile digit (Fig. 2a). Chela width should be measured between the first and second spines below the joint of

the mobile digit (Fig. 2a). Chela height should be measured at the same location as chela width (Fig. 2b).

Measurement order:

Left chela first, right chela next.

For each chela, length first, width second, and height third.

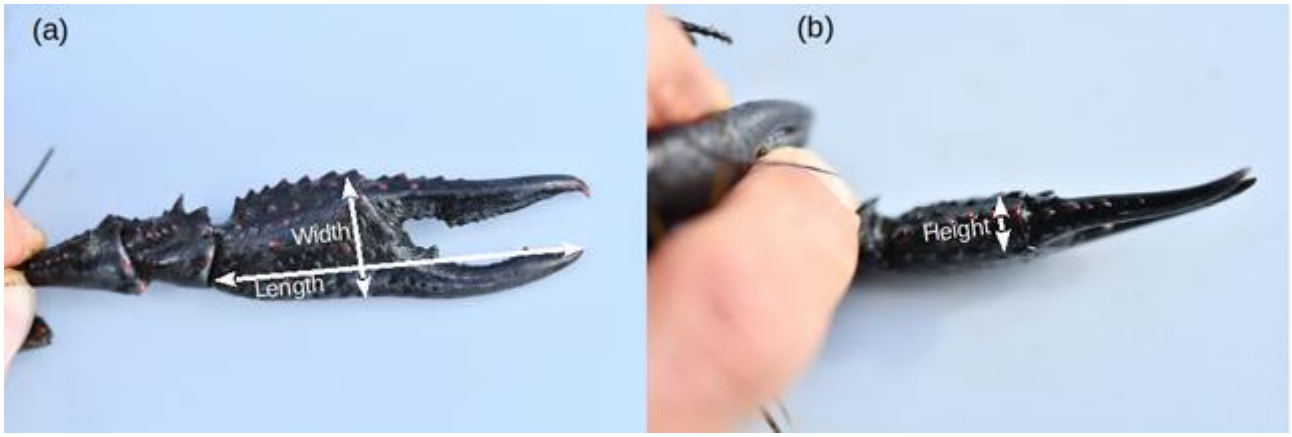

Fig.2. Crayfish chela. **(a)**: Positions of length and width measurements. **(b)**: Position of height measurement.

If chela are absent, atrophied or damaged see below.

DAMAGED ROSTRUM (Total length and cephalothorax length)

Take an approximate length measurements using tip of exopodite of antenna (Figs. 3a and 3b) and write as a remark “Damaged rostrum, approximate measurements”.

“NA” values for total length should be recorded only when the cephalothorax or abdomen is destroyed.

“NA” values for cephalothorax length should be recorded only when the cephalothorax is destroyed.

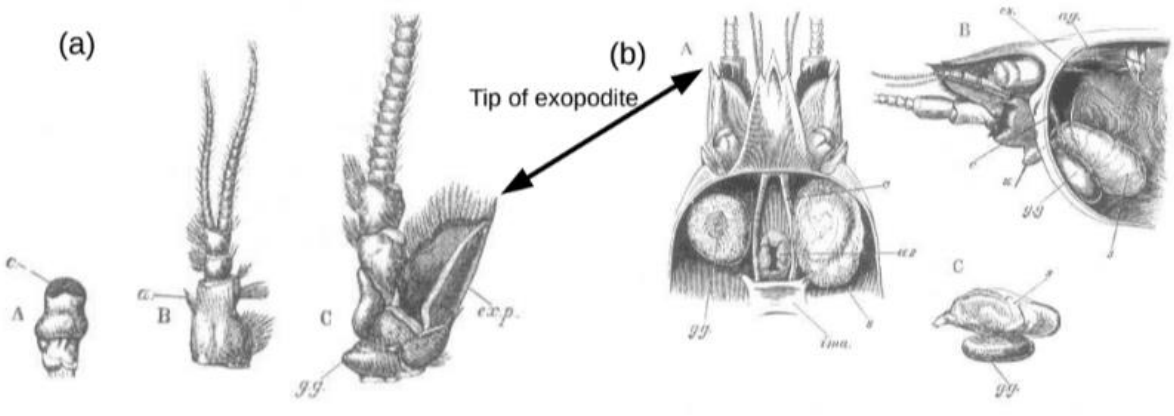

Fig. 3. (a): *Astacus fluviatilis*.--A, eye-stalk; B, antennule; C, antenna of the left side (x 3). a, spine of the basal joint of the antennule; c, corneal surface of the eye; exp, exopodite or squame of the antenna; gg, aperture of the duct of the green gland. **(b)**: Astacus fluviatilis.--A, the anterior part of the body, with the dorsal portion of the carapace removed to show the position of the green glands; B, the same, with the left side of the carapace removed; C, the green gland removed from the body (all x 2). ag, left anterior gastric muscle; c, circumoesophageal commissures; cs, cardiac portion of stomatch; gg, green gland, exposed in A on the left side by the removal of its sac; ima, intermaxillary or cepalic apodeme; oes, oesophagus seen in transverse section in A, the stomach being removed; s, sac of green gland; x, bristle passed from the aperture in the basal joint of the antenna into the sac.

CHELA ABSENT

A <u>0 value</u> should be recorded for each of chela length, width and height.

ATROPHIED CHELA

<u>Measure</u> chela length, width and height as indicated in Fig. 2, and write “Atrophied chela” in the remarks.

BROKEN CHELA

<u>Measure</u> chela length as indicated in Fig. 2, and write “Broken chela” in the remarks.

APPENDIX C - State-Space Model

```
model {
  #priors and constraints
  r0 ~ dnorm(1.0, 0.001)
  beta1 ~ dnorm(0.0, 0.001)
  beta2 ~ dnorm(0.0, 0.001)
  beta3 ~ dnorm(0.0, 0.001)
  for(i in 1:nPop){
   epsilon[i] ~ dnorm(0.0, 1/pow(sigma.epsilon, 2))
  }
  sigma.epsilon ~ dunif(0.0, 100.0)
  #Likelihood
   for(i in 1:nPop) {
    logN.est[i,1] ~ dunif(log(39.9), log(40.1))
      # State process
      for(t in 1:(T-1)) {
       r[i,t] <-    r0 + beta1 * temp[t] + beta2 * (logN.est[i, t] - mean(logN.est[i, t])) + beta3 * difftime[t]
+ epsilon[i]
       logN.est[i, t+1] <- logN.est[i, t] + r[i,t]
      }
    # Observation process
    for(t in 1:T) {
      y[i,t] ~ dnorm(logN.est[i,t], 1/pow(sigma.log.obs[i,t]+1e-6, 2))
    } }
   #Population size on real scale
```

```
  for(i in 1:nPop){
    for (t in 1:T) {
      N.est[i,t] <- exp(logN.est[i,t])
    } } }
```

The parameters temp[t] (temperature) and difftime[t] (time-interval) were centered around zero when constructing the data bundle for the JAGS mode.